DTU Library

An omnibus likelihood test statistic and its factorization for change detection in time series of polarimetric SAR data

Nielsen, Allan Aasbjerg; Conradsen, Knut; Skriver, Henning

Published in:
Proceedings of the 2016 Conference on Big Data From Space (BiDS '16)

Link to article, DOI:
10.2788/854791

Publication date:
2016

Document Version
Peer reviewed version

Citation (APA):
Nielsen, A. A., Conradsen, K., & Skriver, H. (2016). An omnibus likelihood test statistic and its factorization for change detection in time series of polarimetric SAR data. In Proceedings of the 2016 Conference on Big Data From Space (BiDS '16) (pp. 316-319). Publications Office of the European Union. https://doi.org/10.2788/854791

AN OMNIBUS LIKELIHOOD RATIO TEST STATISTIC AND ITS FACTORIZATION FOR CHANGE DETECTION IN TIME SERIES OF POLARIMETRIC SAR DATA

Allan Aasbjerg Nielsen[a], Knut Conradsen[a], and Henning Skriver[b]

Technical University of Denmark
[a]DTU Compute – Applied Mathematics and Computer Science
[b]DTU Space – National Space Institute
DK-2800 Kgs. Lyngby, Denmark

ABSTRACT

Based on an omnibus likelihood ratio test statistic for the equality of several variance-covariance matrices following the complex Wishart distribution with an associated p-value and a factorization of this test statistic, change analysis in a short sequence of multilook, polarimetric SAR data in the covariance matrix representation is carried out. The omnibus test statistic and its factorization detect if and when change(s) occur. The technique is demonstrated on airborne EMISAR L-band data but may be applied to Sentinel-1, Cosmo-SkyMed, TerraSAR-X, ALOS and RadarSat-2 or other dual- and quad/full-pol, and even single-pol data also.

1. INTRODUCTION

In earlier publications we have described a test statistic for the equality of two variance-covariance matrices following the complex Wishart distribution with an associated p-value [1]. We showed their application to bitemporal change detection and to edge detection [2] in multilook, polarimetric synthetic aperture radar (SAR) data in the covariance matrix representation. The test statistic and the associated p-value is described in [3] also. In [4] we focused on the block-diagonal case, we elaborated on some computer implementation issues, and we gave examples on the application to change detection in both full and dual polarization bitemporal, bifrequency, multilook SAR data.

In [5] we described an omnibus test statistic Q for the equality of $k \geq 2$ variance-covariance matrices following the complex Wishart distribution. We also described a factorization of $Q = \prod_{j=2}^{k} R_j$ where Q and R_j determine if and when a difference occurs. Additionally, we gave p-values for Q and R_j. Finally, we demonstrated the use of Q and R_j and the p-values to change detection in truly multitemporal, full polarization SAR data.

For more references to change detection in polarimetric SAR data, see [5].

The methods may be applied to other polarimetric SAR data also such as data from Sentinel-1, COSMO-SkyMed, TerraSAR-X, ALOS, and RadarSat-2 and also to single-pol data.

2. TEST STATISTICS AND THEIR DISTRIBUTIONS

This section gives the main results from [5]. The average covariance matrix for multilook polarimetric SAR is defined as [6]

$$\langle \boldsymbol{C} \rangle = \begin{bmatrix} \langle S_{hh}S_{hh}^* \rangle & \langle S_{hh}S_{hv}^* \rangle & \langle S_{hh}S_{vv}^* \rangle \\ \langle S_{hv}S_{hh}^* \rangle & \langle S_{hv}S_{hv}^* \rangle & \langle S_{hv}S_{vv}^* \rangle \\ \langle S_{vv}S_{hh}^* \rangle & \langle S_{vv}S_{hv}^* \rangle & \langle S_{vv}S_{vv}^* \rangle \end{bmatrix}$$

where $\langle \cdot \rangle$ denotes ensemble averaging and * denotes complex conjugation. S_{rt} denotes the complex scattering amplitude for receive and transmit polarization ($r, t \in \{h, v\}$ for horizontal and vertical polarization).

2.1. Test for equality of several complex covariance matrices

To test whether a series of $k \geq 2$ complex variance-covariance matrices $\boldsymbol{\Sigma}_i$ are equal, i.e., to test the null hypothesis

$$H_0 : \ \boldsymbol{\Sigma}_1 = \boldsymbol{\Sigma}_2 = \cdots = \boldsymbol{\Sigma}_k$$

against all alternatives, we use the following omnibus test statistic (for the real case see [7]; for the case with two complex matrices see [1,2]; $|\cdot|$ denotes the determinant)

$$Q = \left\{ k^{pk} \frac{\prod_{i=1}^{k} |\boldsymbol{X}_i|}{|\boldsymbol{X}|^k} \right\}^n .$$

Here the $\boldsymbol{\Sigma}_i$ (and the $\boldsymbol{X}_i$) are p by p ($p = 3$ for full pol data, $p = 2$ for dual pol data, and $p = 1$ for single channel power data), and the $\boldsymbol{X}_i = n\hat{\boldsymbol{\Sigma}}_i = n\langle \boldsymbol{C} \rangle_i$ follow the complex Wishart distribution, i.e., $\boldsymbol{X}_i \sim W_C(p, n, \boldsymbol{\Sigma}_i)$. n is the equivalent number of looks. Further, $\boldsymbol{X} = \sum_{i=1}^{k} \boldsymbol{X}_i \sim W_C(p, nk, \boldsymbol{\Sigma})$. If the hypothesis is true ("under H_0" in statistical parlance), $\hat{\boldsymbol{\Sigma}} = \boldsymbol{X}/(kn)$. $Q \in [0, 1]$ with $Q = 1$ for equality.

Fig. 1. RGB images of diagonal elements of the L-band data March, April, May (top row, left to right), June, July, August (bottom row, left to right).

For the logarithm of the test statistic we get

$$\ln Q = n\left\{pk\ln k + \sum_{i=1}^{k}\ln|\boldsymbol{X}_i| - k\ln|\boldsymbol{X}|\right\}.$$

A simple expression for the probability of finding a smaller value of $-2\ln Q$ is ($z = -2\ln q_{\text{obs}}$)

$$P\{-2\ln Q \le z\} \simeq P\{\chi^2((k-1)p^2) \le z\}.$$

A better a approximation for P can be obtained. Setting

$$\begin{aligned} f &= (k-1)p^2 \\ \rho &= 1 - \frac{(2p^2-1)}{6(k-1)p}\left(\frac{k}{n} - \frac{1}{nk}\right) \\ \omega_2 &= \frac{p^2(p^2-1)}{24\rho^2}\left(\frac{k}{n^2} - \frac{1}{(nk)^2}\right) - \frac{p^2(k-1)}{4}\left(1 - \frac{1}{\rho}\right)^2 \end{aligned}$$

the probability of finding a smaller value of $-2\rho\ln Q$ is ($z = -2\rho\ln q_{\text{obs}}$)

$$\begin{aligned} P\{-2\rho\ln Q \le z\} &\simeq P\{\chi^2(f) \le z\} \\ &+ \omega_2[P\{\chi^2(f+4) \le z\} - P\{\chi^2(f) \le z\}]. \end{aligned}$$

$P\{-2\rho\ln Q \le -2\rho\ln q_{\text{obs}}\} = P\{Q \ge q_{\text{obs}}\}$ is the change probability, $1 - P\{-2\rho\ln Q \le -2\rho\ln q_{\text{obs}}\} = P\{Q < q_{\text{obs}}\}$ is the no-change probability.

2.2. Test for equality of first $j < k$ complex covariance matrices

If the above test shows that we cannot reject the hypothesis of equality, no change has occurred over the time span covered by the data. If we can reject the hypothesis, change has occurred at some time point. To test whether the first j complex variance-covariance matrices $\boldsymbol{\Sigma}_i$ are equal, i.e., given that

$$\boldsymbol{\Sigma}_1 = \boldsymbol{\Sigma}_2 = \cdots = \boldsymbol{\Sigma}_{j-1}$$

then the likelihood ratio test statistic R_j for testing the hypothesis

$$H_{0,j} : \boldsymbol{\Sigma}_j = \boldsymbol{\Sigma}_1 \ \text{ against } \ H_{1,j} : \boldsymbol{\Sigma}_j \ne \boldsymbol{\Sigma}_1$$

is

$$R_j = \left\{\frac{j^{jp}}{(j-1)^{(j-1)p}}\frac{|\boldsymbol{X}_1 + \cdots + \boldsymbol{X}_{j-1}|^{(j-1)}|\boldsymbol{X}_j|}{|\boldsymbol{X}_1 + \cdots + \boldsymbol{X}_j|^j}\right\}^n$$

Table 1. Part of the change analysis structure for an example with data from six time points.

	$t_1 = \cdots = t_6$	$t_2 = \cdots = t_6$	$t_3 = \cdots = t_6$	$t_4 = \cdots = t_6$	$t_5 = t_6$
Omnibus	$Q^{(1)}$: $P\{Q^{(1)} < q^{(1)}_{\rm obs}\}$	$Q^{(2)}$: $P\{Q^{(2)} < q^{(2)}_{\rm obs}\}$	$Q^{(3)}$: $P\{Q^{(3)} < q^{(3)}_{\rm obs}\}$	$Q^{(4)}$: $P\{Q^{(4)} < q^{(4)}_{\rm obs}\}$	$Q^{(5)}$: $P\{Q^{(5)} < q^{(5)}_{\rm obs}\}$
$t_1 = t_2$	$R^{(1)}_2$: $P\{R^{(1)}_2 < z^{(1)}_{2,\rm obs}\}$				
$t_2 = t_3$	$R^{(1)}_3$: $P\{R^{(1)}_3 < z^{(1)}_{3,\rm obs}\}$	$R^{(2)}_2$: $P\{R^{(2)}_2 < z^{(2)}_{2,\rm obs}\}$			
$t_3 = t_4$	$R^{(1)}_4$: $P\{R^{(1)}_4 < z^{(1)}_{4,\rm obs}\}$	$R^{(2)}_3$: $P\{R^{(2)}_3 < z^{(2)}_{3,\rm obs}\}$	$R^{(3)}_2$: $P\{R^{(3)}_2 < z^{(3)}_{2,\rm obs}\}$		
$t_4 = t_5$	$R^{(1)}_5$: $P\{R^{(1)}_5 < z^{(1)}_{5,\rm obs}\}$	$R^{(2)}_4$: $P\{R^{(2)}_4 < z^{(2)}_{4,\rm obs}\}$	$R^{(3)}_3$: $P\{R^{(3)}_3 < z^{(3)}_{3,\rm obs}\}$	$R^{(4)}_2$: $P\{R^{(4)}_2 < z^{(4)}_{2,\rm obs}\}$	
$t_5 = t_6$	$R^{(1)}_6$: $P\{R^{(1)}_6 < z^{(1)}_{6,\rm obs}\}$	$R^{(2)}_5$: $P\{R^{(2)}_5 < z^{(2)}_{5,\rm obs}\}$	$R^{(3)}_4$: $P\{R^{(3)}_4 < z^{(3)}_{4,\rm obs}\}$	$R^{(4)}_3$: $P\{R^{(4)}_3 < z^{(4)}_{3,\rm obs}\}$	$R^{(5)}_2$: $P\{R^{(5)}_2 < z^{(5)}_{2,\rm obs}\}$

Table 2. Average no-change probabilities for the grass field.

	$t_1 = \cdots = t_6$	$t_2 = \cdots = t_6$	$t_3 = \cdots = t_6$	$t_4 = \cdots = t_6$	$t_5 = t_6$
Omnibus	0.0003	0.0010	0.0210	0.0653	0.0791
$t_1 = t_2$	0.2753				
$t_2 = t_3$	0.0171	0.0784			
$t_3 = t_4$	0.0341	0.0895	0.2688		
$t_4 = t_5$	0.0015	0.0048	0.0309	0.1287	
$t_5 = t_6$	0.3565	0.3016	0.2184	0.1521	0.0791

or

$$\ln R_j = n\{p(j \ln j - (j-1)\ln(j-1)) + (j-1)\ln|\sum_{i=1}^{j-1} \boldsymbol{X}_i| + \ln|\boldsymbol{X}_j| - j\ln|\sum_{i=1}^{j} \boldsymbol{X}_i|\}.$$

Furthermore, the R_j constitute a factorization of Q

$$Q = \prod_{j=2}^{k} R_j$$

or $\ln Q = \sum_{j=2}^{k} \ln R_j$. If H_0 is true the R_j are independent. A simple expression for the probability of finding a smaller value of $-2\ln R_j$ is ($z_j = -2\ln r_{j,\rm obs}$)

$$P\{-2\ln R_j \le z_j\} \simeq P\{\chi^2(p^2) \le z_j\}.$$

A better a approximation for P can be obtained. Letting

$$\begin{aligned} f &= p^2 \\ \rho_j &= 1 - \frac{2p^2-1}{6pn}\left(1 + \frac{1}{j(j-1)}\right) \\ \omega_{2j} &= -\frac{p^2}{4}\left(1 - \frac{1}{\rho_j}\right)^2 \\ &\quad + \frac{1}{24n^2}p^2(p^2-1)\left(1 + \frac{2j-1}{j^2(j-1)^2}\right)\frac{1}{\rho_j^2} \end{aligned}$$

we get ($z_j = -2\rho_j \ln r_{j,\rm obs}$)

$$P\{-2\rho_j \ln R_j \le z_j\} \simeq P\{\chi^2(f) \le z_j\} + \omega_{2j}[P\{\chi^2(f+4) \le z_j\} - P\{\chi^2(f) \le z_j\}].$$

3. CHANGE VISUALIZATION EXAMPLES

To illustrate the above we use full polarimetry EMISAR [8,9] L-band data acquired in 1998 over a Danish agricultural test site on $t_1 = 21$ March, $t_2 = 17$ April, $t_3 = 20$ May, $t_4 = 16$ June, $t_5 = 15$ July, and $t_6 = 16$ August. Figure 1 shows the diagonal elements of the covariance matrix. $\langle S_{hv}S^*_{hv}\rangle$ (red) is stretched linearly between –36 dB and –6 dB, $\langle S_{hh}S^*_{hh}\rangle$ (green) between –30 dB and 0 dB and $\langle S_{vv}S^*_{vv}\rangle$ (blue) between –24 dB and 0 dB. The darker areas in the March and April images are bare surfaces corresponding to spring crops, and the very bright areas in all images are forest areas, primarily coniferous forest. The development of the crops during the growing season is clearly seen in the series of images from March to August.

Table 1 shows the change structure built (for each pixel) for an example with data from six time points. The first column indicates which tests are performed for the row in question. The second column shows $Q^{(1)}$ and $P\{Q^{(1)} < q_{\rm obs}\}$ ("Omnibus" row), or $R^{(1)}_j$ and $P\{R^{(1)}_j < r_{j,\rm obs}\}$, $j = 2,\ldots,6$ for all time points t_1 through t_6. The third column shows $Q^{(2)}$ and $P\{Q^{(2)} < q_{\rm obs}\}$ ("Omnibus" row), or $R^{(2)}_j$ and $P\{R^{(2)}_j < r_{j,\rm obs}\}$, $j = 2,\ldots,5$ for time points t_2 through t_6. The fourth column shows $Q^{(3)}$ and $P\{Q^{(3)} < q_{\rm obs}\}$ ("Omnibus" row), or $R^{(3)}_j$ and $P\{R^{(3)}_j < r_{j,\rm obs}\}$, $j = 2,\ldots,4$ for time points t_3 to t_6, etc. Remember, that for a test for $R^{(\ell)}_j$ to be valid, all previous tests for $R^{(\ell)}_i$, $i = 2,\ldots,j-1$ must show equality, see hypothesis $H_{0,j}$ in Section 2.2.

Note, that $R^{(\ell)}_2$ are the (marginal, non-omnibus) pairwise tests for equality.

(a) $-2\rho \ln Q$

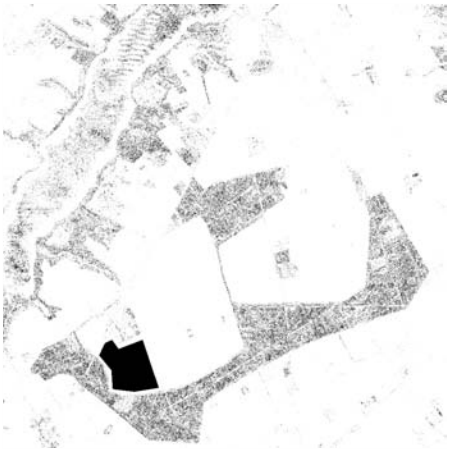

(b) p-value

Fig. 2. Test statistic (a) and p-value with grass field marked as black (b). Dark areas are no-change. p is approximately 1 in the grass field.

3.1. Per pixel change visualization

As examples of per pixel change visualization, Figure 2 shows the quantity $-2\rho \ln Q$ and the corresponding p-value, i.e., the change probability. Figure 3 shows changes from t_1 to t_2 as blue, from t_3 to t_4 as green, and from t_5 to t_6 as red after applying a 3 by 3 mode filter. Black areas have not changed.

3.2. Per field change visualization

Table 2 shows the average no-change probabilities for the grass field shown in Figure 2. Table 2 shows that the pairwise tests reveal no change over time for the grass field (p-values are 0.2753, 0.0784, 0.2688, 0.1287 and 0.0791, respectively). The omnibus test statistic Q indicates change at some time point between March and August ($P\{Q^{(1)} < q^{(1)}_{\mathrm{obs}}\} = 0.0003$), and the R_j show that the first change for this field occurs between April and May

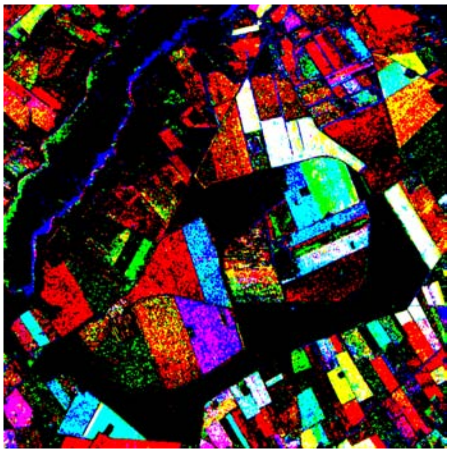

Fig. 3. Shows changes from t_1 to t_2 as blue, from t_3 to t_4 as green, from t_5 to t_6 as red (after application of a 3 by 3 mode filter); change probability significance level is 99.99%.

($P\{R^{(1)}_3 \leq r^{(1)}_{3,\mathrm{obs}}\} = 0.0171$). The second and last change for this field occurs between June and July ($P\{Q^{(2)} < q^{(2)}_{\mathrm{obs}}\} = 0.0010$ and $P\{R^{(2)}_4 \leq r^{(2)}_{4,\mathrm{obs}}\} = 0.0048$).

4. REFERENCES

[1] K. Conradsen, A. A. Nielsen, J. Schou, and H. Skriver, "A test statistic in the complex Wishart distribution and its application to change detection in polarimetric SAR data," *IEEE Transactions on Geoscience and Remote Sensing*, vol. 41, no. 1, pp. 4–19, Jan. 2003, http://www.imm.dtu.dk/pubdb/p.php?1219.

[2] J. Schou, H. Skriver, A. A. Nielsen, and K. Conradsen, "CFAR edge detector for polarimetric SAR images," *IEEE Transactions on Geoscience and Remote Sensing*, vol. 41, no. 1, pp. 20–32, Jan. 2003, http://www.imm.dtu.dk/pubdb/p.php?1224.

[3] M. J. Canty, *Image Analysis, Classification and Change Detection in Remote Sensing,with Algorithms for ENVI/IDL and Python*, Taylor & Francis, CRC Press, third revised edition, 2014.

[4] A. A. Nielsen, K. Conradsen, and H. Skriver, "Change detection in full and dual polarization, single- and multi-frequency SAR data," *IEEE Journal of Selected Topics in Applied Earth Observations and Remote Sensing*, vol. 8, no. 8, pp. 4041–4048, Aug. 2015, http://www.imm.dtu.dk/pubdb/p.php?6827.

[5] K. Conradsen, A. A. Nielsen, and H. Skriver, "Determining the points of change in time series of polarimetric SAR data," *Accepted for IEEE Transactions on Geoscience and Remote Sensing*, 2015, http://www.imm.dtu.dk/pubdb/p.php?6825.

[6] J. J. van Zyl and F. T. Ulaby, "Scattering matrix representation for simple targets," in *Radar Polarimetry for Geoscience Applications*, F. T. Ulaby and C. Elachi, Eds. Artech, Norwood, MA, 1990.

[7] T. W. Anderson, *An Introduction to Multivariate Statistical Analysis*, John Wiley, New York, third edition, 2003.

[8] S. N. Madsen, E. L. Christensen, N. Skou, and J. Dall, "The Danish SAR system: Design and initial tests," *IEEE Transactions on Geoscience and Remote Sensing*, vol. 29, pp. 417–476, 1991.

[9] E. L. Christensen, N. Skou, J. Dall, K. Woelders, J. H. Jørgensen, J. Granholm, and S. N. Madsen, "EMISAR: An absolutely calibrated polarimetric L- and C-band SAR," *IEEE Transactions on Geoscience and Remote Sensing*, vol. 36, pp. 1852–1865, 1998.